

# Synthesis of New Triaryamine-based Polyimides for Electrochromic Applications

Hui-Min Wang (王惠民), Sheng-Huei Hsiao (蕭勝輝)\*

Department of Chemical Engineering and Biotechnology, National Taipei University of Technology  
(國立臺北科技大學化學工程與生物科技系)

Tel: +886-2-27712171 ext. 2548; Fax: +886-2-27317117

E-mail: [shhsiao@ntut.edu.tw](mailto:shhsiao@ntut.edu.tw)

## Abstract

Four new main-chain triphenylamine-based polyimides were prepared from the polycondensation reactions of diamine monomers, *N,N*-bis(4-aminophenyl)-*N',N'*-bis(4-*tert*-butylphenyl)-1,4-phenylenediamine (**1**) and 4,4'-diamino-4''-(3,6-di-*tert*-butylcarbazol-9-yl)triphenylamine (**1'**), with pyromellitic dianhydride (PMDA) and 1,4,5,8-naphthalenetetracarboxylic dianhydride (NTDA), respectively. These polyimides showed high glass transition temperatures and high thermal stability. Cyclic voltammetry studies revealed that these polyimides were ambipolar; they showed well-defined and reversible redox couples during both p- and n-doping processes, together with multi-electrochromic behaviors and high contrast ratios in the visible and near-infrared regions. An electrochromic device (ECD) based on polypyromellitimide **3a** is also constructed and characterized. The device shows a maximum optical contrast ( $\Delta T\%$ ) of 85% at 940 nm for green coloring and of 91% at 760 nm for dark blue coloring.

## 1. Introduction

Research in electrochromic devices (ECDs) has received a great deal of attention due to the importance of this phenomenon in applications such as electrochromic windows, displays, anti-glare mirrors, eye-glasses and solar-attenuated windows.[1] In general, four major classes of materials are used to construct ECDs, including metal oxides, inorganic coordination complexes, molecular dyes, and conjugated polymers.[2]. Among the different types of electrochromic materials, conjugated polymers such as polyanilines, polypyrroles, polyselenophenes, polythiophenes, and in particular, poly(3,4-ethylenedioxythiophene) (PEDOT) and its derivatives attract increasing interest because of mechanical flexibility, ease in band-gap/color-tuning via structural control, and the potential for low-cost processing for large-area devices.[3] For efficient operation of an electrochromic device, it is necessary to take a number of properties into consideration: electrochromic efficiency, optical contrast, response time, stability and durability. The difficulty in achieving satisfactory values for all these parameters at the same time stimulates the development of new methods of preparation of electrochromic films, new materials and components for the devices.

Aromatic polyimides are commercially important materials used extensively in a wide range of optoelectronic applications due to their excellent chemical, thermal, and dielectric properties.[4] Despite their outstanding properties, most of the conventional aromatic polyimides have high melting or glass-transition temperatures ( $T_g$ ) and limited solubility in most organic solvents because of their rigid backbones and strong interchain interactions. One of the common approaches for increasing solubility and processability of polyimides without sacrificing high thermal stability is the introduction of bulky, packing-disruptive groups into the polymer backbone.[5] Incorporation of three-dimensional, packing-disruptive triarylamine units into the polyimide backbone not only resulted in enhanced solubility but also led to new electronic functionality of polyimides, such as electrochromic [6] and memory [7] characteristics, due to the redox-activity of the triarylamino core. Recent studies have demonstrated that aromatic polyamides containing *N,N,N',N'*-tetraphenylphenylenediamine (TPPA) or (3,6-di-*tert*-butylcarbazol-9-yl)TPA segments show attractive electrochromic properties such as high coloration

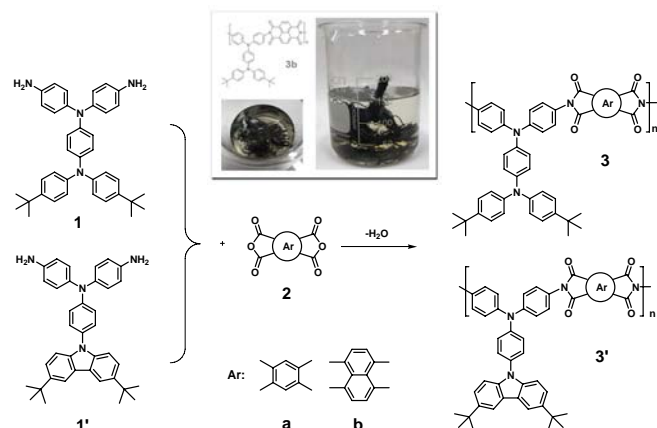
efficiency, high optical contrast, fast response time, long-term cycling stability, and multicolored electrochromism.[8] The radical cations of these polyamides generally showed rather strong bands in the near infrared (NIR) region due to a mixed-valence-type transition (charge transfer transition between pairs of chromophores in different oxidation states).[9]

Aromatic imide dyes, especially perylenediimides, have been used as n-type semiconductors and electron acceptors in many fundamental studies of organic electronics including molecular switches and wires,[10] solar energy conversion devices,[11] n-channel thin film transistors,[12] and electrochromic or light-emitting devices.[13] These molecules have been used in electron-transfer studies because they undergo reversible one-electron reduction at modest potentials to form stable anion radicals localized on the electron deficient units. The electrochemical and spectroscopic properties of different imides, diimides and polyimides have been extensively studied.[14] The most important electrochemical property of aromatic diimide-based compounds, such as pyromellitimides, naphthalenediimides and perylenediimides, is the existence of a stable anion radical and dianion reduced states. Thin layers of polyimides with the above-mentioned diimide units on electrodes are known to be electrochromic and undergo electrically reversible color change between the three redox states (neutral, radical anion, and dianion). In this paper, we successfully synthesized two polypyromellitimides (PPIs **3a** and **3'a**) and two polynaphthalimides (PNIs **3b** and **3'b**) from the polycondensation reactions of the triphenylamine-based diamines **1** and **1'** with pyromellitic dianhydride (PMDA; **2a**) and 1,4,5,8-naphthalenetetracarboxylic dianhydride (NTDA; **2b**), respectively. The optoelectronic properties of these polyimides have been measured and discussed. This study suggests that these polyimides are ambipolar multi-electrochromic materials with high redox stability during the oxidation process. An ECD based on PPI **3a** is also constructed and characterized. The device shows good electrochromic stability and high optical contrast ratios.

## 2. Synthesis and basic characterization of polyimides

PPIs **3a** and **3'a** were prepared by the polycondensation reactions of diamines **1** and **1'**, respectively, with PMDA (**2a**) via a conventional two-step process, that is, the formation of a poly(amic acid) and subsequent thermal or chemical imidization (Scheme 1). The poly(amic acid) precursors of **3a** and **3'a** had inherent viscosities of 1.11 and 1.36 dL/g in DMAc and could be cast into a flexible and tough poly(amic acid) film, which could be subsequently converted into a tough polyimide film by extended heating at elevated temperatures. The poly(amic acid) precursor also could be chemically dehydrated to the polyimide by treatment with acetic anhydride and pyridine. PNIs **3b** and **3'b** was prepared by a one-pot, high-temperature solution polymerization of diamines **1** and **1'**, respectively, with NTDA (**2b**) in *m*-cresol at 180 °C in the presence of isoquinoline as catalyst. PNIs **3b** and **3'b** exhibited inherent viscosities of 0.51 and 0.60 dL/g, respectively, in *m*-cresol. All the polyimides could afford flexible and tough films via solution casting, indicating they are high molecular weight polymers. The structures of these polyimides were confirmed with IR spectroscopy. PPIs **3a** and **3'a** gave two characteristic bands at around 1780 and 1730  $\text{cm}^{-1}$  (imide asymmetric and symmetric

stretching), whereas PNIs **3b** and **3'b** showed the imide absorptions at around 1720 and 1675  $\text{cm}^{-1}$  due to a less strained six-membered ring.



**Scheme 1.** Synthesis and structures of polyimides **3** and **3'**.

The thermal properties of the polyimides were investigated by TGA and DSC techniques. These polyamides exhibited good thermal stability with no remarkable weight loss up to 450  $^{\circ}\text{C}$  in nitrogen or in air. Their decomposition temperatures ( $T_d$ ) at a 10 % weight-loss in nitrogen and air were recorded at 525–594 and 472–582  $^{\circ}\text{C}$ , respectively. The carbonized residue (char yield) of the polymers was more than 48 % at 800  $^{\circ}\text{C}$  in nitrogen atmosphere, ascribed to their high aromatic content. These polyimides not only showed good thermal stability but also possessed remarkably high glass-transition temperatures ( $T_g$ ) of 281–364  $^{\circ}\text{C}$ . The thermal analysis results revealed that these polyimides exhibited excellent thermal stability, which in turn is beneficial to increase the service time in device application and enhance the morphological stability to the spin-coated films.

### 3. Electrochemical properties

The electrochemical behavior of each polyimide was investigated by CV using a conventional three-electrode cell assembly. The CV diagrams of all the polyimides are depicted in Fig. 1, and quantitative details are summarized in Table 1. All the polyimides underwent a reversible two-electron oxidation and reduction, revealing their high-electrochemical stability for both p- and n-doping (ambipolar) process. The redox waves observed during the anodic sweep can be attributed to the formation of radical cations and dications originated from the oxidation processes of the TPPA and (3,6-di-*tert*-butylcarbazol-9-yl)TPA units (Scheme 2). It is also worth noting that polyimides **3a** and **3b** with TPPA unit reveals a lower oxidation potential ( $E_{1/2}^{\text{Ox}1} = 0.74, 0.65 \text{ V}$  and  $E_{1/2}^{\text{Ox}2} = 1.10, 1.03 \text{ V}$ ) compared to polyimides **3'a** and **3'b** ( $E_{1/2}^{\text{Ox}1} = 0.99 \text{ V}$  and  $E_{1/2}^{\text{Ox}2} = 1.27, 1.33 \text{ V}$ ) with carbazole-substituted TPA unit. This could be attributed to the fact that the pendent 4,4'-di-*tert*-butyl TPA unit is easier to oxidize than the 3,6-di-*tert*-butyl-9-phenylcarbazole unit.

The CV of PPIs **3a** and **3'a** (Fig. 1a and 1c) show that the pyromellitimide groups undergo two quasi-reversible one-electron reductions, which occurred at  $E_{pc} = -0.75 \sim -0.80$  and  $-1.35 \text{ V}$ . The first reduction corresponds to formation of radical anions, and the second reduction relates to formation of dianions.[14b] The electrochemical behavior of PNIs **3b** and **3'b** shown in Fig. 1b and 1d have two redox couples at more positive potentials than that for PPIs **3a** and **3'a**. The results are similar to that reported by Viehbeck et al.[14b] The extended aromatic fused ring will increase the resonance energy and delocalize the negative charge more effectively. Therefore, the first one-electron reduction potential of PNIs **3b** and **3'b** are less negative than that of PPIs **3a** and **3'a**. For

polyimides **3a** and **3'b**, the proposed sequential oxidation reactions and reduction reaction for generation of the radical anions and cations are shown in Scheme 3. The dianion form of polyimides **3b** and **3'b** are represented by reduced *cis*-carbonyls. It can also be represented by reduced *trans*-carbonyls, but this requires the loss of aromaticity in the naphthalene unit.[13a]

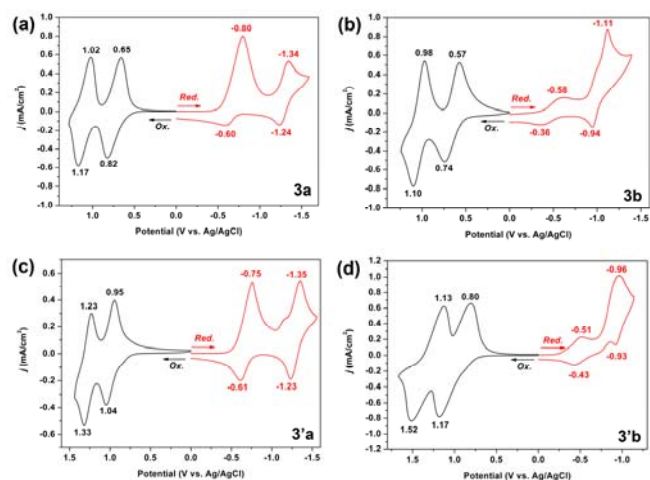


**Fig. 1.** Cyclic voltammetric diagrams of the cast films of polyimides (a) **3a**, (b) **3b**, (c) **3'a**, and (d) **3'b** on an ITO-coated glass substrate in 0.1 M  $\text{Bu}_4\text{NClO}_4/\text{acetonitrile}$  (for p type doping) and DMF (for n type doping) solution at a scan rate of 50 mV/s, respectively.

### 4. Spectroelectrochemistry

The electro-optical properties of the polymer films were investigated using the changes in electronic absorption spectra at various applied voltages. For these investigations, the polyimide film was cast on an ITO-coated glass slide (a piece that fit in the UV-vis cuvette), and a homemade electrochemical cell was built from a commercial UV-vis cuvette. The cell was placed in the optical path of the sample light beam in a commercial diode array spectrophotometer. This procedure allowed us to obtain electronic absorption spectra under potential control in a 0.1 M  $\text{Bu}_4\text{NClO}_4/\text{acetonitrile}$  or DMF solution. The results of the **3a** film upon oxidation and reduction is presented in Fig. 2 as a series of UV-vis-NIR absorption curves correlated to electrode potentials. In the neutral form the film exhibits a strong band at 317 nm characteristic for  $\pi-\pi^*$  transitions, but it was almost transparent in the visible and NIR regions. The band gap of polymer **3a** was calculated as 2.74 eV from the onset of the  $\pi-\pi^*$  transition at 452 nm. Upon electro-oxidation of the **3a** film (increasing applied voltage from 0 to 0.9 V), the absorption of  $\pi-\pi^*$  transition at 317 nm gradually decreased while a new absorption peak at 414 nm and a broadband having its maximum around 886 nm in the NIR region grew up. We attribute this spectral change to the formation of a stable monocation radical from the TPPA moiety. The absorption band in the NIR region is assigned to an intervalence charge-transfer (IV-CT) between states in which the positive charge is centered at different amino centers.[9] Upon further oxidation at applied voltages to 1.5 V, the intensity of the IV-CT band gradually decreased, with a formation of a new strong absorption band centered at about 685 nm. We attribute these spectral changes to the formation of a stable dication of the TPPA moiety. The observed electronic absorption changes in the film of **3a** at various potentials are fully reversible and are associated with strong color changes; indeed, they even can be seen readily by the naked eye. From the photos shown in bottom of Fig. 2a, it can be seen that the film changed from a transmissive neutral state (nearly colorless;  $L^*$ , 90;  $a^*$ , 1;  $b^*$ , 1) to a highly absorbing semi-oxidized state (yellow;  $L^*$ , 61;  $a^*$ , -2;  $b^*$ , 11 and green;  $L^*$ , 43;  $a^*$ , -6;  $b^*$ , 4)

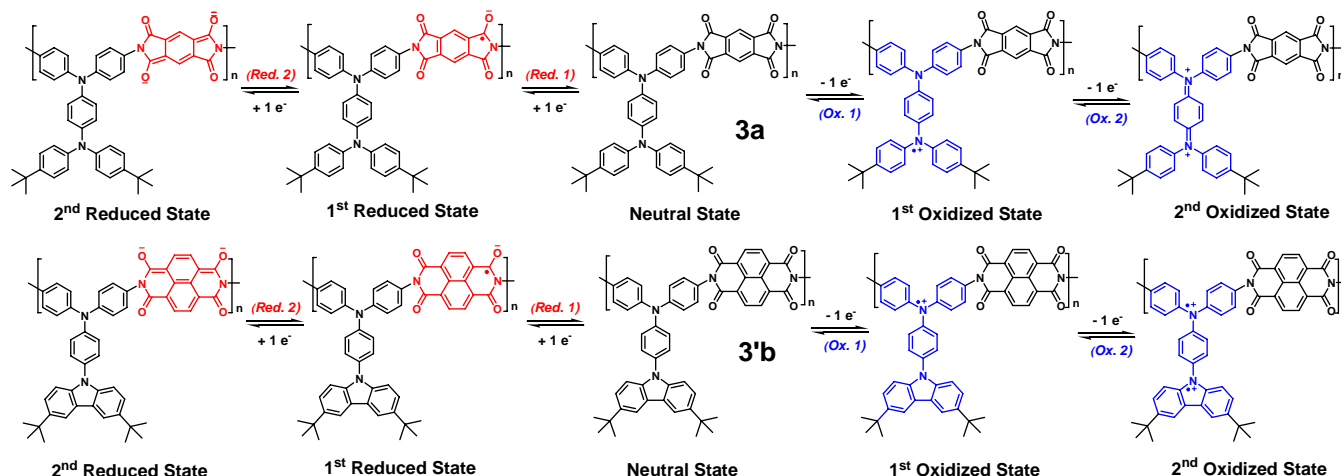
and a fully oxidized state (blue;  $L^*$ , 38;  $a^*$ , -8;  $b^*$ , -4). **Figs. 2b** and **2c** show the spectral changes of the **3a** film upon reduction. The radical anion **3a<sup>-•</sup>**, which appears at potentials between -0.5 and -0.8 V vs. Ag/AgCl, exhibits a strong band at 330 nm and two peaks in the visible region (a stronger band at 724 nm with a weaker one at 657 nm). As shown in the inset of **Fig. 2b**, the radical anion form of polyimide **3a** is pale green ( $L^*$ , 65;  $a^*$ , -6;  $b^*$ , -3) in color. Further reduction at potentials below -1.45 V results in the two-electron reduced (dianion) state with a new peak at 564 nm, and the film turns to a red-violet ( $L^*$ , 54;  $a^*$ , 25;  $b^*$ , -18) color during the second reduction (**Fig. 2c**). The spectral changes associated with

the reduction reactions of the pyromellitimide unit are very similar to that of standard PMDA-ODA polyimide (ODA: 4,4'-oxydianiline) reported by Mazur et al.[14a] This result reaffirms that the diamine residue has very little direct influence on the reduction of the diimide moiety as reported by Mazur et al.[14a] Photographs and  $L^*a^*b^*$  color coordinates of all the polyimide films at various redox states are summarized in **Fig. 3**. These multicolored electrochromic behavior suggest that these novel TPA-based polyimides have great potential for electrochromic applications.

**Table 1.** Redox Potentials and Energy Levels of Polyimides

Code	Thin films (nm)		Oxidation Potential <sup>a</sup> (V)			Reduction Potential <sup>b</sup> (V)			Bandgap <sup>c</sup> (eV)		Energy Levels <sup>d</sup> (eV)	
	$\lambda_{\max}$	$\lambda_{\text{onset}}$	$E_{\text{onset}}$	$E_{1/2}^{\text{Ox1}}$	$E_{1/2}^{\text{Ox2}}$	$E_{\text{onset}}$	$E_{1/2}^{\text{Red1}}$	$E_{1/2}^{\text{Red2}}$	$E_g^{\text{opt}}$	$E_g^{\text{eg}}$	HOMO	LUMO
<b>3a</b>	310	452	0.60	0.74	1.10	-0.55	-0.70	-1.29	2.74	1.44	5.10	3.66
<b>3b</b>	307, 346, 363	409	0.55	0.65	1.03	-0.36	-0.50	-1.03	3.03	1.15	5.01	3.86
<b>3'a</b>	298, 315,	407	0.86	0.99	1.27	-0.55	-0.68	-1.29	3.04	1.67	5.35	3.68
<b>3'b</b>	298, 345, 365	407	0.85	0.99	1.33	-0.34	-0.50	-1.00	3.04	1.49	5.35	3.86

<sup>a</sup> vs. Ag/AgCl in CH<sub>3</sub>CN.  $E_{1/2}$  = average potential of the redox couple peaks. <sup>b</sup> vs. Ag/AgCl in DMF. <sup>c</sup> Bandgaps calculated from absorption edge of the polymer films:  $E_g^{\text{opt}} = 1240/\lambda_{\text{onset}}$ ;  $E_g^{\text{eg}} = E_{\text{HOMO}} - E_{\text{LUMO}}$ . <sup>d</sup>  $E_{\text{HOMO}} = -(E_{1/2}^{\text{Ox1}} + 4.8)$  (eV);  $E_{\text{LUMO}} = -(E_{1/2}^{\text{Red1}} + 4.8)$  (eV)



**Scheme 2.** Proposed redox chemistry of the polyimides **3a** and **3'b**

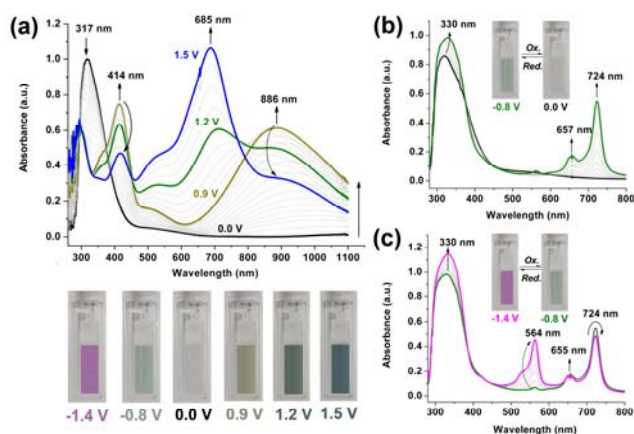


**Fig. 2** Spectral changes of the cast film of polyimide **3a** on the ITO-coated glass substrate on (a) p-doping in 0.1 M Bu<sub>4</sub>NClO<sub>4</sub>/CH<sub>3</sub>CN and (b, c) n-doping in 0.1 M Bu<sub>4</sub>NClO<sub>4</sub>/DMF at various applied potentials (vs. Ag/AgCl). The photographs show the color change of the film on an ITO electrode at indicated potentials.

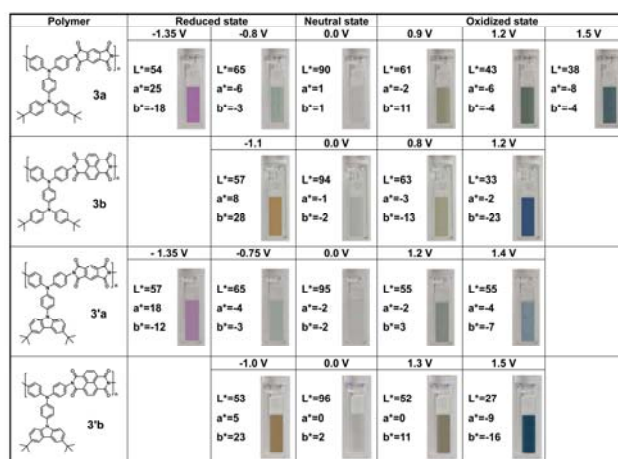


**Fig. 3**  $L^*a^*b^*$  color coordinates and photograph of the polyimide films at various redox states.

## 7. Electrochromic devices

Finally, we fabricated as preliminary investigations single layer electrochromic cells (Fig. 4b). The polyimide films were spray-coated onto ITO-glass and then dried. Afterwards, the gel electrolyte was spread on the polymer-coated side of the electrode and the electrodes were sandwiched. To prevent leakage, an epoxy resin was applied to seal the device. As a typical example, an electrochromic cell based on polyimide **3a** was fabricated. The polymer film is pale yellow in neutral form. When the voltage was increased (to a maximum of 2.5 V), the color changed from colorless (neutral) to green (semi-oxidized) and dark blue (fully oxidized), the same as was already observed for the solution spectroelectrochemistry experiments. As show in Fig. 4a, the electrochromic device shows a high optical contrast both in the visible and NIR regions with a transmittance change ( $\Delta T$ ) of 85% at 940 nm for green coloring at electrode potential of 2.0 V and 91% at 760 nm for blue coloring at electrode potential of 2.5 V. When the potential was subsequently set back at 0 V, the polymer film turned back to original pale yellow. We believe that optimization could further improve the device performance and fully explore the potential of these electrochromic polyimides.

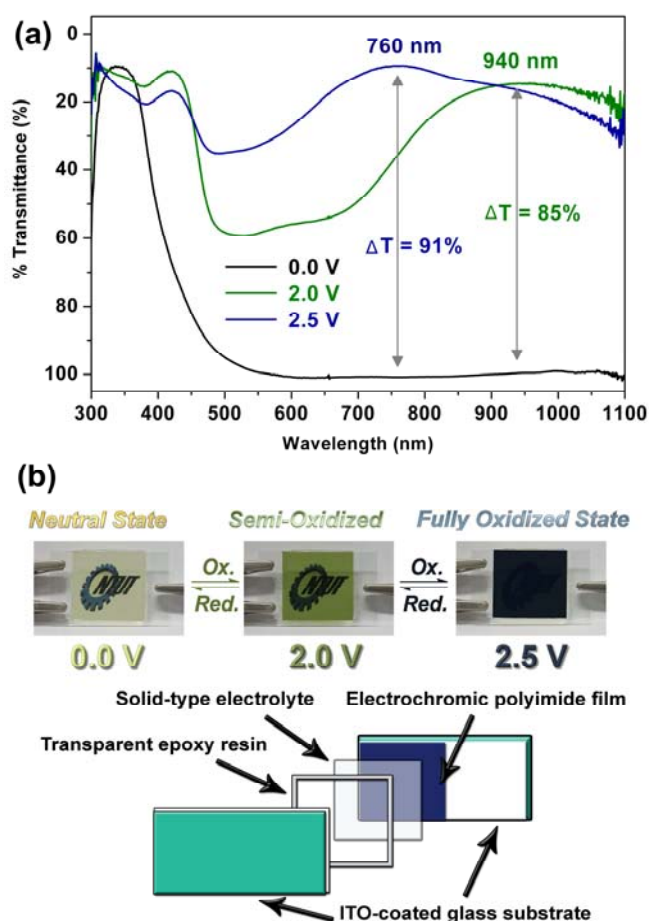


**Fig. 4** (a) Transmittance spectra of single-layer ITO-coated glass ECD, using polyimide **3a** as active layer. (b) Photographs and schematic diagram of polyimide EDC.

## 7. Conclusions

We have successfully prepared four new triphenylamine-containing redox-active polyimides and demonstrated that these polymers show high  $T_g$ , and ambipolar and multicolored electrochromic behavior. Electrochemical and spectral results showed that these polymers can be employed as potential

anodically and cathodically coloring materials in the development of electrochromic devices. Further development of materials of this type would seem to be warranted by the encouraging initial results presented here.

## References

- [1] P. M. S. Monk, R. J. Mortimer and D. R. Rosseinsky, *Electrochromism and Electrochromic Devices*, Cambridge University Press, Cambridge, UK, 2007.
- [2] P. M. Beaujuge and J. R. Reynolds, *Chem. Rev.*, 2010, **110**, 268–320.
- [3] (a) M. Icli, M. Pamuk, F. Algi, A. M. Onal and A. Cihaner, *Chem. Mater.*, 2010, **22**, 4034–4044; (b) E. Sefer, F. B. Koyuncu, E. Oguzhan and S. Koyuncu, *J. Polym. Sci., Part A: Polym. Chem.*, 2010, **48**, 4419–4427.
- [4] M. M. Ghosh and K. L. Mittal, ed., *Polyimides: Fundamentals and Applications*, Marcel Dekker, New York, 1996.
- [5] (a) Q. Zhang, S.-H. Li, W.-M. Li and S.-B. Zhang. *Polymer* 2007, **48**, 6246–6253; (b) Y.-T. Chern and J.-Y. Tsai. *Macromolecules*, 2008, **41**, 9556–9564.
- [6] (a) S.-H. Cheng, S.-H. Hsiao, T.-H. Su and G.-S. Liou, *Macromolecules*, 2005, **38**, 307–316; (b) G.-S. Liou, S.-H. Hsiao and H.-W. Chen, *J. Mater. Chem.*, 2006, **16**, 1831–1842; (c) Y.-C. Kung, G.-S. Liou and S.-H. Hsiao, *J. Polym. Sci., Part A: Polym. Chem.*, 2009, **47**, 1740–1755; (d) H.-M. Wang and S.-H. Hsiao, *Polymer*, 2009, **50**, 1692–1699.
- [7] (a) D. M. Kim, S. Park, T. J. Lee, S. G. Halm, K. Kim, J. C. Kim, W. Kwon and M. Ree, *Langmuir*, 2009, **25**, 11713–11719; (b) T. Kuorosawa, C.-C. Chueh, C.-L. Liu, T. Higashihara, M. Ueda and W.-C. Chen, *Macromolecules*, 2010, **43**, 1236–1244.
- [8] (a) S.-H. Hsiao, G.-S. Liou and H.-M. Wang, *J Polym Sci Part A: Polym Chem.*, 2009, **47**, 2330–2343; (b) H.-M. Wang, S.-H. Hsiao, G.-S. Liou and C.-H. Sun, *J. Polym. Sci. Part A: Polym. Chem.*, 2010, **48**, 4775–4789; (c) H.-M. Wang and S.-H. Hsiao, *Polym. Chem.* 2010, **1**, 1013–1023; (d) H.-M. Wang and S.-H. Hsiao, *J. Polym. Sci. Part A: Polym. Chem.*, 2011, **49**, 337–351.
- [9] (a) C. Lambert and G. Noll, *Angew. Chem. Int. Ed.*, 1998, **37**, 2107–2110; (b) C. Lambert and G. Noll, *J. Am. Chem. Soc.*, 1999, **121**, 8434–8442; (c) C. Lambert and G. Noll, *Synth. Met.*, 2003, **139**, 57–62.
- [10] (a) W. P. Debreczeny, W. A. Svec, E. M. Marsh and M. R. Wasielewski, *J. Am. Chem. Soc.*, 1996, **118**, 8174–8175; (b) T. M. Wilson, M. J. Tauber and M. R. Wasielewski, *J. Am. Chem. Soc.*, 2009, **131**, 8952–8957.
- [11] W. A. Angadi, D. Gosztola and M. R. Wasielewski, *J. Appl. Phys.*, 1998, **83**, 6187–6189.
- [12] R. Schmidt, J. H. Oh, Y.-S. Sun, M. Deppisch, A.-M. Krause, K. Radacki, H. Braunschweig, M. Konemann, P. Erk, Z. Bao and F. Wurthner, *J. Am. Chem. Soc.*, 2009, **131**, 6215–6228.
- [13] (a) S. K. Lee, Y. Zu, A. Herrmann, Y. Geerts, K. Mullen and A. J. Bard, *J. Am. Chem. Soc.*, 1999, **121**, 3513–3520; (b) Z. B. Hill, D. B. Rodovsky, J. M. Leger and G. P. Bartholomew, *Chem. Commun.*, 2008, 6594–6596.
- [14] (a) S. Mazur, P. S. Lugg and C. Yarnitzky, *J. Electrochem. Soc.*, 1987, **134**, 346–353; (b) A. Viehbeck, M. J. Goldberg and C. A. Kovac, *J. Electrochem. Soc.*, 1990, **137**, 1460–1466; (c) L. Wang, G. W. Goodloe, B. J. Stallman and V. Cammarata, *Chem. Mater.*, 1996, **8**, 1175–1181; (d) W. Lu, J. P. Gao, Z. Y. Wang, Y. Qi, G. G. Sacripante, J. D. Duff and P. R. Sundararajan, *Macromolecules*, 1999, **32**, 8880–8885; (e) S. M. Mackinnon and Z. Y. Wang, *J. Polym. Sci., Part A: Polym. Chem.*, 2000, **38**, 3467–3475.